Ion Imprinted Polymers Prepared with a Novel Cd(II) Methacrylate Monomer Complex with 1-Vinylimidazole for Selective Removal of Cd(II) Ions

Zuhal Yolcu (zuhal.yolcu@giresun.edu.tr)
Giresun University Arts and Science Faculty https://orcid.org/0000-0001-7761-122X
Meryem Çıtlakoğlu
Giresun University Arts and Science Faculty

Research Article

Keywords: Cd(II)-methacrylate complex, 1-vinylimidazole, crystal structure, ion imprinted polymer, adsorption

Posted Date: March 5th, 2021

DOI: https://doi.org/10.21203/rs.3.rs-271926/v1

Abstract

A novel $[Cd(maa)_2(vim)_2H_2O]\cdot H_2O$ monomer complex was synthesized using methacrylic acid (maaH) and 1-vinylimidazole (vim) that are suitable ligands for polymerization with cadmium central atom. Cd(II)-IIP was prepared by precipitation polymerization technique using monomer complex, EGDMA, and AIBN as functional monomer, crosslinker, and initiator, respectively. The structure of the monomer complex was elucidated by single-crystal X-ray diffraction method. Infrared spectroscopy (FT-IR) and thermogravimetric analysis (TGA) methods were used for characterization both of the monomer complex and Cd(II)-IIP. Scanning electron microscopy / energy-dispersive X-ray spectroscopy (SEM/EDX) methods were used for observation surface morphology and content of the polymer surfaces. The adsorption performance and selectivity properties of Cd(II)-IIP were also investigated. The maximum adsorption capacity of Cd(II)-IIP was 43.0 mg/g with 250 mg/L initial Cd(II) concentration at pH:6.0, and the selectivity was higher for Cd^{2+} ions than that of Pb^{2+}, Ni^{2+}, and Zn^{2+} as competitor ions. The Langmuir and Freundlich isotherm models were applied comparatively to experimental results. Cd(II) ion content of the solutions determined by inductively coupled plasma mass spectrometry (ICP-MS).

1. Introduction

Cadmium is one of the heavy metals on the Environmental Protection Agency's (EPA) list of primary pollutants due to its high toxicity [1-4]. Unlike copper and zinc, cadmium is very harmful to human health even at excessively low concentrations [5-7]. Cadmium is classified as carcinogenic by the International Cancer Research Agency (ICRA) [8-10]. Since cadmium has a high solubility in water, it can discharge into the environmental waters via the waste materials from the Cd-Ni battery producing factories, anthropogenic sources, power stations, and metal planting [11-12]. Thus, it can easily transfer from soil to plants, from plants to the human body [13-14]. The recommendation of World Health Organization (WHO) for Cd(II) ions in drinking water is 3 ng/mL [15]. Therefore, selective separation and elimination of cadmium ions from wastewater have great significance. In recent years, a wide range of chemical and physical treatment methods such as adsorption, ion exchange, membrane treatment, chemical precipitation and electrocoagulation methods have been reported for selective removal of Cd(II) ions from wastewaters [16-17]. Among these methods, the adsorption technique is a highly effective and economical one. Also, many adsorbents such as clays, minerals (calcite), calcareous aggregates, zeolites, dead biomass, or mineral wool were used for the removal of Cd(II) ions from various samples [13, 18-21]. Selective determination of metal ions in real samples is difficult for lots of applications. Over the past decade, ion-imprinted polymers (IIPs) have been developed especially for the recognition of metal ions [22-25]. Among them, the researchers paid special attention to the studies on the development of Cd(II) ion-imprinted polymer, due to the harmful effects of cadmium on living things [2, 4-7, 9-10, 17, 26-30].

The polymer prepared by the ion-imprinting technique possesses good recognized ability to the template ion. The ion-imprinting method has three process steps as complexation, polymerization, and removal of template ions from the polymer. The coordination geometry, coordination number, charges and sizes of metal ions, and the specificity of ligand are important specifications for the selectivity of polymer as

adsorbent [26]. In recent years unsaturated carboxylic acids (acrylic, methacrylic, fumaric, maleic, oleic, crotonic, vinyl benzoic acids) are frequently used as monomers in the imprinted polymer method. The molecules containing vinyl group (-CH=CH_2) such as methacrylic acid (maaH) and 1–vinylimidazole (vim) are used as monomers in the polymerization processes. These polymerizable ligands are used in the synthesis of the metal-containing monomers. The metal-containing monomers are used in the synthesis phase of the polymer to be prepared. Existing carboxylic acid groups increase the variety of metal coordination environments and facilitate the design of new advanced materials [31-32].

In this study, a novel [Cd$(maa)_2(vim)_2H_2O]\cdot H_2O$ complex containing 1-vinylimidazole and methacrylic acid was synthesized as a monomer for preparation of Cd(II) ion-imprinted polymer (Cd(II)-IIP). Then, Cd(II)-IIP was prepared by precipitation polymerization method, in which the monomer complex as a monomer. Except for the synthesized complex, no other monomer was used in the polymer synthesis process The crystal structure of the monomer complex was elucidated by X-ray single crystal technique. Thermal behavior of the complex and the polymers were determined by TG, DTG, and DTA techniques. Metal adsorption performance and selectivity properties of Cd(II)-IIP were also investigated.

2. Material And Methods

2.1. Reagents

Cadmium carbonate (Cd(CO_3), methacrylic acid (maaH), 1-vinylimidazole (vim), ethylene glycol dimethacrylate (EGDMA), methyl alcohol, toluene, 2,2'-azobisisobutyronitrile (AIBN), nitric acid, hydrochloric acid, ammonia solution, and other salts were purchased obtained from Sigma Aldrich Ltd. SPC Science brand standards were used for adsorption and pH studies.

2.2. Apparatus

A Costech ECS 4010 model instrument was used for elemental analysis of the monomer complex. FT-IR analysis was conduct by using a Jasco FT/IR-6600 typeA model spectrophotometer. Thermogravimetric analyzes were carried out using a TA Instruments SII O-EXSTAR 6000 model thermo-gravimetric/differential thermal analyzer (TG/DTA). The reflection intensities of the monomer complex were collected by using a Bruker D8 QUEST model diffractometer. SEM-EDX analysis was performed with a Hitachi SU 1510 model instrument. A Bruker brand 820 MS model ICP-MS spectrometer was used for metal determinations. A Denver instruments UB-7 (USA) model pH meter was used for pH measurements.

2.3. Preparation of Cd(II)-methacrylate complex

In order to Cd(II)-methacrylate complex, 8 mmol of maa ligand dissolved in the solution 20 mL of MeOH/H_2O 50:50 (v/v) was added over 4 mmol of Cd(CO_3) in 10 mL of distilled water and stirred for 1 hour. A solution of 4 mmol vim ligand dissolved in 5 mL of MeOH was added and stirred for another 1 hour and

allowed to crystallize. After 3 days, transparent stick crystals were obtained. Anal. Calc. for $C_{18}H_{24}CdN_4O_5 \cdot H_2O$: C, 42.65; H, 4.77; N, 11.05. Found: C, 42.86; H, 4.55; N, 10.86%.

2.4. Preparation of Cd(II)-IIP

The preparation scheme of Cd(II)-IIP was shown in Fig. 1. Primarily Cd(II)-methacrylate monomer complex 250 mg was dissolved in 6 mL of methanol. 10 mL of 2:3 (v/v) EGDMA toluene solution was added to first solution. 40 mg of AIBN was dissolved in the polymerization mixture deoxygenated with N_2 gas for 15 min. N_2 gas was passed through another balloon containing 30 mL of methanol for 15 min to remove the oxygen and heated to 60 ℃ in a thermostatic regulated oil bath. The polymerization mixture was added into the flask containing methanol and the polymerization was completed at 60 ℃ under magnetic stirring for 24 h. After filtration, the polymer beads were washed with 1:1 (v/v) ethanol:water solution. Then, dried polymer was washed with 0.5 M HCl to ensure the removal of the Cd(II) ions from the polymer. Finally, the polymer (Cd-IIP) was washed with deionized water, until the filtrate was neutralized and dried at room temperature. Also, NIP particles were prepared in the absence of monomer complex.

2.5. Characterization methods of Cd(II)-methacrylate complex and Cd(II)-IIP

FT-IR and TGA methods were used for characterizations of both the monomer complex and Cd(II)-IIP. Also, single-crystal X-ray diffractometry and SEM-EDX methods were specifically used for characterizations of the monomer complex and Cd(II)-IIP, respectively. The morphologies of the Cd(II)-IIP particles were observed by SEM, and also the determination of the presence of Cd(II) ion in Cd(II)-IIP was performed using EDX methods. TGA experiments were carried out from 30 to 800 ℃ (heating rate: 10 ℃ min^{-1}, sample weight: 3 mg, N_2 atmosphere). The reflection intensities of the complex were collected at 296 K with graphite-monochromated Mo-Kα radiation (l=0,71073 Å). The structure was solved using SHELXT [33] by direct methods, and all non-hydrogen atoms were refined with anisotropic displacement parameters by full-matrix least-squares methods on F^2 using SHELXL [34] from within the WINGX [35]. The MERCURY program was used for molecular graphics [36]. Supramolecular analyses were made with the PLATON [37]. The details about the crystal data and structure determination are summarized in Table 1. Selected bond lengths, bond angles and hydrogen-bond geometry are given in Table S1.

2.6. Adsorption procedure

The adsorption performances of the Cd(II)-IIP were investigated via batch sorption experiments. The initial concentration and pH effect on the adsorption were investigated. Standard solutions (50 mg/L

concentration of Cd(II) ions) were adjusted to the demanded pH levels (pH range 2.0–7.0) by using a pH-meter with the additions of HNO_3 or NH_3 solutions. 50 mg of Cd(II)-IIP was added into a conical flask that contained 20 mL of Cd(II) solution with 50 mg/L concentration. The mixture was mechanically shaken for 24 h, at 25 ℃. The absorbance of the filtrate was measured at ICP-MS and the amount of metal ion adsorbed by the polymer was calculated according to the quantity of Cd(II) left in the filtrate.

The adsorption capacity of Cd(II)-IIP was also investigated by batch experiments for different initial Cd(II) ion concentrations ranging from 10 to 300 mg/L at pH:6,0. The adsorption capacity of Cd(II)-IIP was calculated from the following equation:

$$Q = \frac{(C_0 - C)V}{m} \quad (1)$$

where Q is the adsorption capacity of Cd(II)-IIPs, mg/g. C_0 and C are the initial and final concentrations of cadmium ions in aqueous solution, mg/L, respectively. V represents the volume of aqueous solution, L; m represent the weight of Cd(II)-IIP, g.

Competitive adsorptions of Pb(II), Ni(II), and Zn(II) in the presence of Cd(II) were investigated by batch experiments. 50 mg of Cd(II)-IIP or NIP were treated with 20 mL (pH 6.0) of a solution of these competitive ions (100 mg/L for each one). The distribution ratio and the selectivity factor of the ions were calculated using the following equations:

$$K_d = \frac{(C_0 - C)V}{mC} \quad (2)$$

$$k = \frac{K_d(Cd^{2+})}{K_d(M^{2+})} \quad (3)$$

where M^{2+}represents competitive metal ions, K_d and k are distribution ratio and selectivity factor, respectively.

3. Results And Discussion

3.1. Characterization of Cd(II)-methacrylate monomer complex

According to the single crystal X-ray diffraction analysis, the complex crystallized in the orthorhombic system with space group *Pnna* (Table 1.). The crystal structure of the monomer complex with the atom labeling is shown in Fig. 2. The two maa acts as a bidentate ligand and vim is monodentate ligand coordinated to the metal via its tertiary nitrogen atom. The Cd(II) ion has seven coordinates by the two nitrogen atoms (N1 and $N1^i$) from the two vim, four oxygen atoms (O1, $O1^i$, O2, and $O2^i$) from two maa,

and one oxygen (O3w) from an aqua ligand. Thus, Cd(II) ion display distorted pentagonal bipyramid geometry. In crystallization, an uncoordinated water molecule is also part of the unit cell.

In the complex, the Cd1—O1 and Cd1—O2 bond lengths are 2.524(2) and 2.373(3) Å, the Cd1—O3W bond length is 2.334(4) Å, and the Cd1—N1 bond length is 2.289(2) Å. Further, N1-Cd1-$N1^{i}$ bond angle is 169.77(14)°, O1—Cd1—$O1^{i}$ and O2—Cd1—$O2^{i}$ bond angles are 174.81(12)° and 81.30(12)°, respectively (Table S1., see Supplementary Data). The values of the complex are normal and comparable with the complexes in the literature [38-40].

Table 1. Crystal data and refinement parameters for $[Cd(maa)_2(vim)_2H_2O]\cdot H_2O$ complex

Crystal data	
Empirical formula	$C_{18}H_{24}CdN_4O_5 \cdot H_2O$
Formula weight	506.83
Temperature (K)	296
Crystal system	Orthorhombic
Space Group	Pnna
a, *b*, *c* (Å)	8.7850 (5), 15.2082 (9), 17.2115 (10)
Volume ($A^{\circ 3}$), Z	2089.0(4), 4
Radiation type	Mo *Kα*
Crystal size (mm)	0.19 × 0.15 × 0.13
($D_{celcld,}$ (g cm^{-3}))	1.576
Absorpt. coeff. (μ (mm^{-1}))	0.99
Data collection	
Diffractometer	Bruker *APEX*-II CCD
Absorption correction	Multi-scan Bruker
*T*min, *T*max	0.618, 0.746
No. of measured, independent and observed [$I > 2\sigma(I)$] reflections	47097, 2859, 2144
*R*int	0.055
(sin θ/λ)max ($Å^{-1}$)	0.667
Refinement	
$R[F^2 > 2\sigma(F^2)]$, $wR(F^2)$, *S*	0.046, 0.082, 1.31
No. of reflections	2859
No. of parameters	142
No. of restraints	2
H-atom treatment	H atoms treated by a mixture of independent and constrained

	refinement
$\Delta\rho$max, $\Delta\rho$min (e Å^{-3})	0.41, −0.51

There are strong intra- and intermolecular O—H···O and weak C—H···O and C—H···π interactions in the crystal packing of complex (Fig. 3(a)). Intra molecular hydrogen bond is between H atom of uncoordinated water and O atom of maa and the distance O4···O2^{iii} is 2.787 Å (Fig. 3(b)). Intermolecular hydrogen bond O3—H3···O1^{ii} giving rise to $R_2^2(8)$ ring motifs is between aqua and maa (Fig. 3(b)). Another intermolecular hydrogen bond C5—H5···O1^{i} is between vim and maa, where the vim donate H atoms to the neighboring maa O atoms (Fig. 3(c)). The distances O3···O1^{ii} and C5···O1^{i} are 2.732 and 3.260 Å, respectively. The C8—H8···π interaction is between H atom of vim and the neighboring imidazole rings [C8—H8···π, d = 2.911 Å and 150°] (Fig. 4). The 3D crystal structure of the complex is formed by H-bonds and van der Walls interactions. Fig. 3(a) shows the packing structure of the complex along the b direction.

FT-IR spectral analysis provides important information for rationalizing the mechanism of the interactions between ligands and metal ion. FT-IR spectrums of $[Cd(maa)_2(vim)_2H_2O]\cdot H_2O$ complex, maaH, and vim ligand are shown in Fig.5. The narrow band at 3464 cm^{-1} is attributed to υ(O–H) stretching of uncoordinated water and broadband at 3222 and 3147 cm^{-1} are assigned to υ(O–H) of coordinated aqua ligand [41-42]. The peaks corresponding to asymmetric and symmetric υ(C=O) stretching bands of the methacrylic acid were observed at lower frequencies as 1527 and 1416 cm^{-1} for the complex indicating that the methacrylic acid coordination with the Cd(II) ion via the oxygen atoms of the carboxylate group. The difference (Δυ) between the asymmetric and symmetric carboxylate stretching vibrations is used to determine the coordination type of carboxylate group. The calculated (Δυ) value [υ_{asym}(COO) - υ_{sym}(COO)] of 111 cm^{-1} for the complex is suitable for bidentate coordination (Δυ < 200 cm^{-1}), which is in line with reported previously [38, 43-44]. The peaks at 3113, 3011 and 2923cm^{-1} in the complex attributed to the aromatic, vinylic and aliphatic υ(C-H) stretching vibrations of ligands respectively [45-46]. The absorption band at 1647 cm^{-1} in the complex belongs to C=C band.

The thermal behavior of the complex, whose TGA curves are shown in Fig. 6, was investigated by simultaneous TG-DTA in the temperature range 30–800 ℃ under the nitrogen atmosphere. The Cd(II) complex decomposes in three main steps. The first stage associated with the loss of the aqua ligand and the uncoordinated water molecule occurs between 47 and 104 ℃ (DTG_{max}: 50 and 91 ℃) with a mass loss of 7.64% (Calcd: 7.11%). After this step is related to the degradation of two vim ligand and two maa ligand in the second (104-248 ℃, DTG_{max}: 169 ℃) and third step (248- 511℃, DTG_{max}: 408 ℃) with a

mass loss of 66.85% (Calcd: 67.56 %). The total remaining weight calculations (25.51%) suggested that the final product at 700 ℃ was identified as CdO (Calcd: 25.34%).

3.2. Characterization of Cd(II)-IIP

The surface structure image of the Cd(II)-IIP and NIP were evaluated by SEM. Fig. 7 show structural differences of the before and after elution IIP and NIP, respectively. According to the SEM images shown in Fig. 7 (a) and (b), it was observed that the eluted Cd(II)-IIP had a rougher surface area than the non-eluted Cd(II)-IIP. In addition in Fig. 7(c) NIP particles are quite small in size and have dust form in contrast to the IIP particles.

The energy dispersive X-ray (EDX) analysis of Cd(II)-IIP before and after elution and NIP are shown in Fig. 7. The EDX analysis was used to determine the content of the polymer surfaces, and complete removal of Cd(II) ion from Cd(II)-IIP. The datas in Fig. 7(a) approve the entity of C, O, and Cd in the polymer structure. According to Figure 7 (b), it was observed that the Cd(II) ion was not present in the structure of the Cd(II)-IIPs after elution, showing that the elution of the Cd(II) ion was successfully.

Fig. 8 represents FT-IR spectrums of the Cd(II)–IIP's before and after elution. As can be seen from Fig. 8, both spectrums are similar, indicating that the elution did not cause deterioration on the polymer. The strong bands observed at 1726 and 1151 cm-1 for Cd(II)-IIP before elution, corresponding to C=O and C-O groups, respectively (Fig.8(a)). These peaks moved to 1719 and 1137 cm^{-1} after elution. It means that the Cd(II) ions have been removed successfully. Additionally, when the FT-IR spectrums of the complex (Fig. 5) and polymers (Fig. 8) are compared, it can be seen that the peaks of the carboxyl groups are different. It means that the coordination interaction of Cd(II) ion and carboxyl group strongly changed when Cd(II)-IIP formed.

The thermal behaviors of the Cd(II)-IIP were investigated by TG analysis. As can be seen from TGA curves, degradation of the Cd(II)-IIP before elution (Fig. 9(a)) occur in one step, indicating that 96% of the polymer was decomposed in the range of 152-715 ℃ (DTG_{max}=408 ℃). Similarly, degradation of the Cd(II)-IIP after elution (Fig.9(b)) occur in one step, indicating that 100% of the polymer was decomposed in the range of 229-503 ℃ (DTG_{max}=425 ℃). The Cd(II)-IIP before and after elution showed different residue yields of 4% and 0%, respectively. The residue yield of Cd(II)-IIP before elution was higher than that of Cd(II)-IIP after elution, clearly indicating that the completely removal of Cd(II) ions from the polymer.

3.3. Batch Adsorption Experiments

3.3.1. pH Effect

The pH is an important parameter effected on the amount of the adsorption in aqueous solution. The pH effect on the adsorption capacity of Cd(II)-IIP has been examined for Cd(II) solutions over the pH range of 2.0 to 7.0. The maximum adsorption value was observed at pH 6.0 (Fig. 10.). The pH effect was not studied over pH 8.0 because of the formation of cadmium hydroxide precipitate [17]. According to the results, adsorption of all pH values was observed, but the highest adsorption was at pH: 6.0 for Cd(II) ion in Cd(II)-IIP particles. For this reason, 6.0 was chosen as optimum pH value for other parameters.

3.3.2. Concentration Effect

The initial concentration effect on adsorption capacity of Cd(II)-IIP was investigated. The adsorption capacities increased gradually from 10 to 250 mg/L initial Cd(II) concentrations (Fig. 11.). At 300 mg/L, adsorption capacity of Cd(II)-IIP decreased due to the driving force effect and three-dimensional network structural expansion [29]. The maximum adsorption capacity of Cd(II)-IIP was calculated as 43.0 mg/g. The results suggest that the Cd(II)-IIP had a high adsorption capacity.

The adsorption capacity of imprinted polymers can be defined by the equilibrium adsorption isotherm, expressed by certain constants related to the surface properties and affinity of the adsorbent. The adsorption isotherms were investigated using the Langmuir and Freundlich isotherm models which are given in the supplementary file. (Table S2, Fig. S1-S2, see Supplementary Data). The results indicate that the adsorption of the Cd(II) ions onto Cd(II)-IIP fitted well the Freundlich adsorption isotherm model.

3.3.3. Selectivity of Cd(II)-IIP

In order to investigate of selectivity of Cd(II)-IIP; Pb(II), Ni(II), and Zn(II) ions are chosen as the competitor ions. The selectivity factor coefficients (k) were calculated using the equation *(2)* and *(3)*. As shown in Table 2., the Kd value of the Cd(II) ion is greater than that of the other ions for Cd(II)-IIP. Also, the selectivity coefficients of Cd(II)-IIP for Cd^{2+}/Pb^{2+}, Cd^{2+}/Ni^{2+} and Cd^{2+}/Zn^{2+} were 2.260, 4.414, and 3.361, respectively.

Table 2. Selective adsorption properties of Cd-IIP and NIP

	Cd(II)-IIP		NIP	
Ions	Kd (L/g)	k	Kd (L/g)	k
Cd(II)	0.166		0.018	
Pb(II)	0.074	2.260	0.051	0.360
Ni(II)	0.038	4.414	0.012	1.539
Zn(II)	0.046	3.361	0.013	1.381

According to these results, it is observed that Cd(II)-IIP exhibits a higher adsorption capacity for Cd(II) than the other ions. This is mainly because the ionic recognition and selectivity of the IIPs influenced by the nature of the metal ion, its coordination geometry, and number [47-48]. Therefore, the size and shape of the imprinted sites of Cd(II)-IIP are suitable for Cd(II) ions, and Cd(II)-IIP has a specific selectivity for Cd(II) in the presence of various competitor metal ions.

4. Conclusions

In this work, a novel $[Cd(maa)_2(vim)_2H_2O]\cdot H_2O$ monomer complex containing polymerizable ligands (maa and vim), and its Cd(II)-ion imprinted polymer were successfully synthesized and characterized by different methods. The structure of the monomer complex was determined in detail by the X-ray diffraction method and FT-IR. The complex crystallizes in the orthorhombic system with space group *Pnna*. Cd(II) ion display distorted pentagonal bipyramid geometry $[CdO_5N_2]$ in the crystal structure. The complex molecules show three-dimensional supramolecular networks by C–H···O, O–H···O, N–H···O, and C–H···π interactions. The SEM-EDX and FT-IR were employed to elucidate the morphology, content of surfaces, and bonding of Cd(II)-IIP. In addition, the thermal behaviors of both the complex and the polymer were analyzed by TGA.

In order to determine the maximum adsorption capacity of the prepared polymer, appropriate pH and initial concentration were investigated. The results indicating that Cd(II)-IIP had maximum adsorption capacity at pH:6, as 43 mg/g. The adsorption isotherms were investigated using the Langmuir and Freundlich isotherm models. The experimental data was described the Freundlich adsorption isotherm model well. The selectivity of Cd(II)-IIP was higher for Cd^{2+} ions than that of Pb^{2+}, Ni^{2+}, and Zn^{2+} as competitor ions. Consequently, the Cd(II)-IIP obtained in this study can be regarded to be a suitable sorbent for the selective removal of Cd(II) ions in wastewater.

Declarations

Acknowledgments

The authors acknowledge support by the Giresun University (Project No: FEN-BAP-C-160317-04). The authors also thank Onur Şahin from Sinop University, Turkey, for the X-ray data collection.

Supplementary Data

Crystallographic data for the structural analysis have been deposited with the Cambridge Crystallographic Data Centre, CCDC No. 2055479. Copies of the data can be obtained, free of charge, on application to CCDC, 12 Union Road, Cambridge CB2 1EZ, UK (fax: +44-1223- 336033 or email: deposit@ccdc.cam.ac.uk). Table S1-S2 and Fig. S1-S2 can be found in supplementary files.

References

1. E. Manahan, Industrial Ecology: Environmental Chemistry and Hazardous Waste, (CRC Press, Lewis Publishers, Boca Raton, 1999), p. 180
2. K. Lu, X.-P. Yan, Anal. Chem. 76, 453-457 (2004)
3. Tan, D. Xiao, J. Hazard. Mater. 164, 1359-1363 (2009)
4. Huang, Y. Chen, F. Zhou, X. Zhao, J. Liu, S. Mei, Y. Zhou, T. Jing, J. Hazard. Mater. 333, 137-143 (2017)
5. Li, H. Jiang, S. Zhang, Talanta, 71, 1487-1493 (2007)
6. Liu, D. Wang, Y. Xu, G. Huang, J. Mater. Sci. 46, 1535-1541 (2011)
7. Zhang, B. Hu, Anal. Chim. Acta, 723, 54-60 (2012)
8. Vainio, E. Heseltine, C. Partensky, J. Wilbourn, Scand. J. Work Environ. Health, 360-363, (1993)
9. Zhai, Y. Liu, X. Chang, S. Chen, X. Huang, Anal. Chim. Acta, 593, 123-128 (2007)
10. Candan, N. Tüzmen, M. Andac, C. A. Andac, R. Say, A. Denizli, Mater. Sci. Eng. C, 29, 144-152 (2009)
11. S. Di Toppi, R. Gabbrielli, Environ. Exp. Bot. 41, 105-130 (1999)
12. Chakravarty, N. S. Sarma, H. P. Sarma, Chem. Eng. Journal 162, 949-955 (2010)
13. Robinson, C. Russell, M. Hedley, B. Clothier, Agric. Ecosyst. Environ. 87, 315-321 (2001)
14. B. Kirkham, Geoderma, 137, 19-32 (2006)
15. Guidelines for Drinking-Water Quality, (World Health Organization, Fourth Edition Incorporating the First Addendum, Geneva, 2017), p.180.
16. S. Berber-Mendoza, R. Leyva-Ramos, P. Alonso-Davila, J. Mendoza-Barron, P. E. Diaz-Flores, J. Chem. Technol. Biotechnol. 81, 966-973 (2006)
17. Xi, Y. Luo, J. Luo, X. Luo, J. Chem. Eng. Data, 60, 3253-3261 (2015)
18. Yavuz, R. Guzel, F. Aydın, İ. Tegin, R. Ziyadanoğulları, Pol. J. Environ. Stud. 16, 467-471 (2007)
19. Ozdes, C. Duran, H. B. Senturk, J. Environ. Manage, 92, 3082-3090 (2011)
20. M. Seo, W. T. Lim, Catal. Today, 204, 179-188 (2013)

21. Hanzlíková, J. Braniša, K. Jomová, M. Fülöp, P. Hybler, M. Porubská, Sep. Purif. Technol. 193, 345-350 (2018)
22. A. Cormack, A. Z. Elorza, J. Chromatogr. B Analyt. Technol. Biomed. Life Sci. 804, 173-182 (2004)
23. P. Rao, R. Kala, S. Daniel, Anal. Chim. Acta, 578, 105-116 (2006)
24. C. Eloi, L. Chabanne, G. R. Whittell, I. Manners, Mater. Today 11, 28-36 (2008)
25. R. Whittell, M. D. Hager, U. S. Schubert, I. Manners, Nat. Mater. 10, 176-188 (2011)
26. Andaç, R. Say, A. Denizli, J. Chromatogr. B, 811, 119-126 (2004)
27. Luliński, P. Kalny, J. Giebułtowicz, D. Maciejewska, P. Wroczyński, Polym. Bull. 71, 1727-1741 (2014)
28. Li, C. Feng, M. Li, Q. Zeng, Q. Gan, H. Yang, Appl. Surf. Sci. 332, 463-472 (2015)
29. Bai, L. Fan, Y. Zhou, Y. Zhang, J. Shi, G. Lv, Y. Wu, Q. Liu, J. Song, J. Appl. Polym. Sci. 134, (2017)
30. Wang, Y. Lin, Y. Li, A. Dolgormaa, H. Fang, L. Guo, J. Huang, J. Yang, J. Inorg. Organomet. Polymer Mater. 29, 1874-1885 (2019)
31. I. Dzhardimalieva, A. D. Pomogailo, Russ. Chem. Rev. 77, 259-301 (2008)
32. S. Abd-El-Aziz, E. A. Strohm, Polymer, 53, 4879-4921 (2012)
33. M. Sheldrick, Acta Crystallogr. Sect. A: Found. Crystallogr. 71, 3-8 (2015)
34. M. Sheldrick, Acta Crystallogr. Sect. C: Cryst. Struct. Commun. 71, 3-8 (2015)
35. J. Farrugia, J. Appl. Crystallogr. 32, 837-838 (1999)
36. F. Macrae, P. R. Edgington, P. McCabe, E. Pidcock, G. P. Shields, R. Taylor, M. Towler, J. van de Streek, J. Appl. Crystallogr. 39, 453-457 (2006)
37. Spek, PLATON: A Multipurpose Crystallographic Tool; (University of Utrecht, Utrecht, The Netherlands, 2005)
38. Valencia-Centeno, F. Ureña-Núñez, V. Sánchez-Mendieta, R. A. Morales-Luckie, R. López-Castañares, L. Huerta, J. Coord. Chem. 61, 1589-1598 (2008)
39. Yolcu, S. Demir, Ö. Andaç, O. Büyükgüngör, Acta Chim. Slov. 63, 646-653 (2016)
40. Yolcu, Erzincan University Journal of Science and Technology, 13, 25-32 (2020)
41. Z. Yeşilel, İ. İlker, M. S. Refat, H. Ishida, Polyhedron, 29, 2345-2351 (2010)
42. N. Golovnev, M. S. Molokeev, I. V. Sterkhova, M. K. Lesnikov, Inorg. Chem. Commun. 97, 88-92 (2018)
43. Wu, W.-M. Lu, F.-F. Wu, X.-M. Zheng, J. Coord. Chem. 57, 805-812 (2004)
44. -J. Cai, W.-J. Jiang, Q. Deng, Z.-S. Peng, Y.-F. Long, H. Liu, M.-L. Liu, J. Coord. Chem. 61, 3245-3252 (2008)
45. Yilmaz, O. Andac, S. Gorduk, Polyhedron, 133, 16-23 (2017)
46. Yilmaz, S. Gorduk, O. Andac, Inorganica Chim. Acta, 469, 154-163 (2018)
47. H. Dam, D. Kim, J. Appl. Polym. Sci. 108, 14-24 (2008)
48. Branger, W. Meouche, A. Margaillan, React. Funct. Polym. 73, 859-875 (2013)

Figures

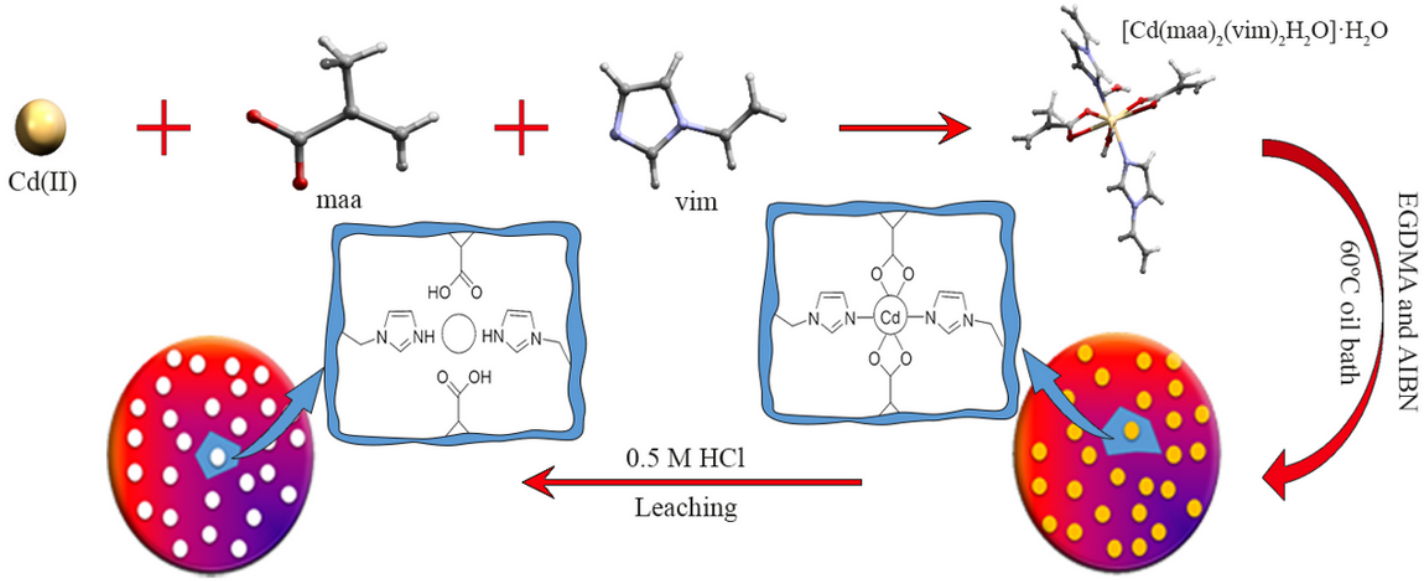

Figure 1

Synthesis scheme of Cd(II)-imprinted polymer

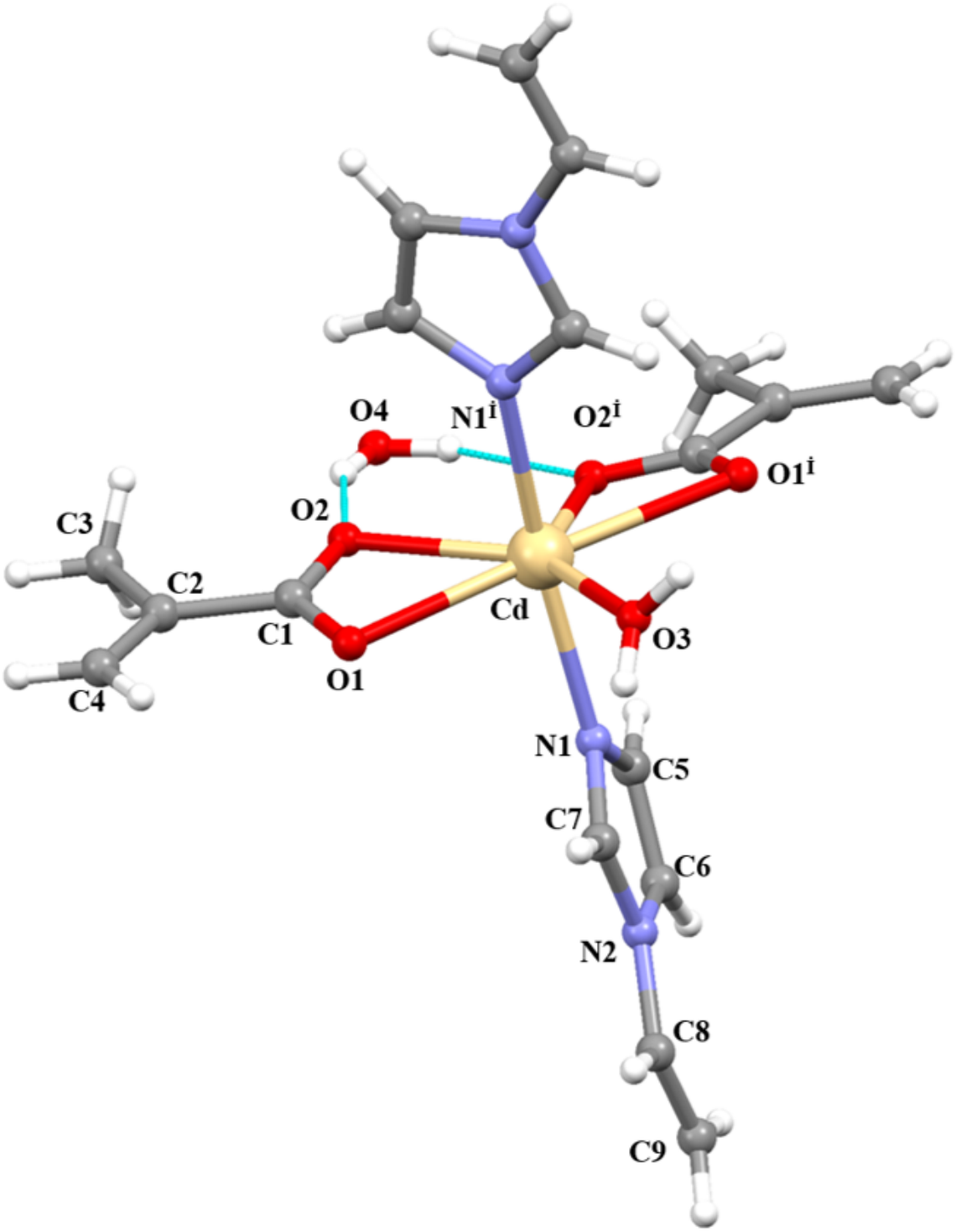

Figure 2

View of the [Cd(maa)2(vim)2H2O]·H2O complex showing the atom-labeling scheme. [(i) −x+1/2, −y+1, z]

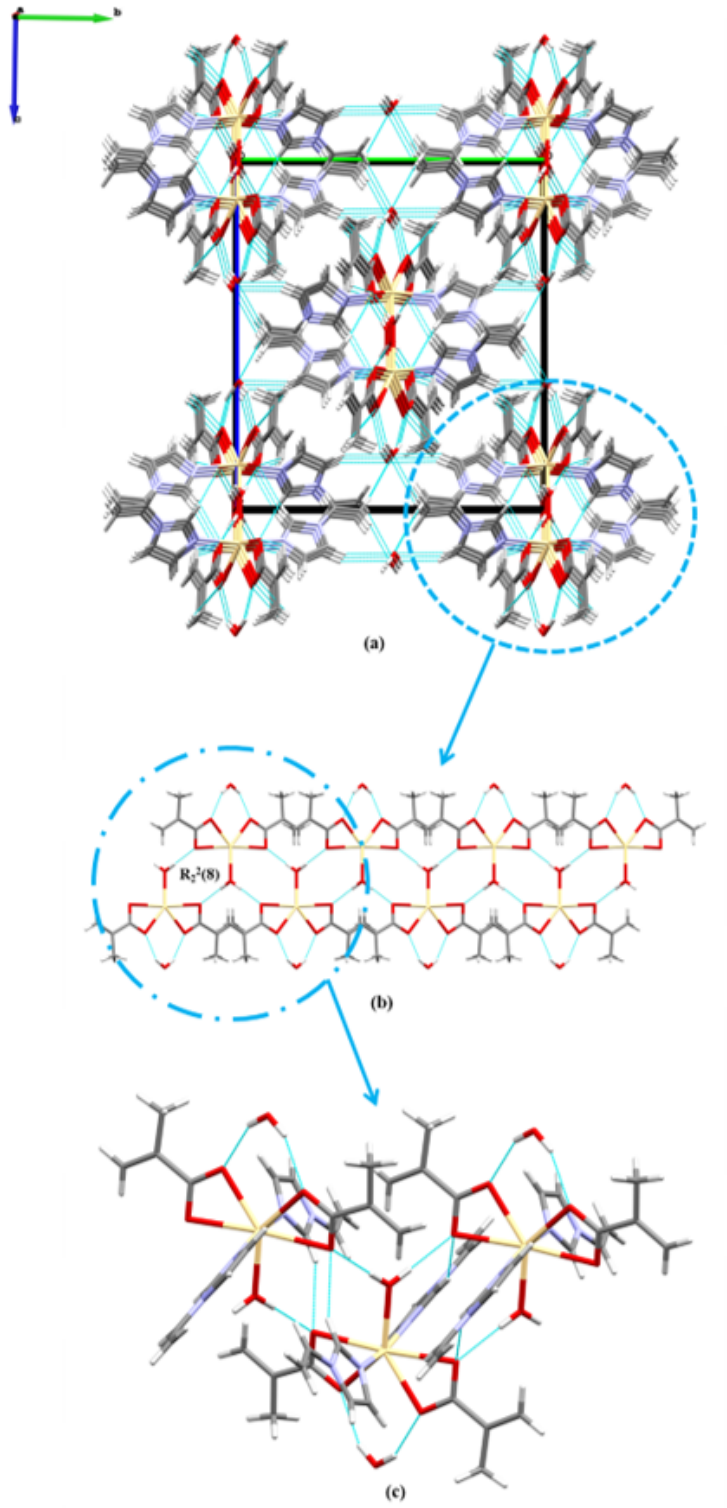

Figure 3

(a) Hydrogen-bonding interaction between the chains of the complex (b) R22 (8) ring motives (c) Intra- and inter-molecular hydrogen-bonding geometry of the complex

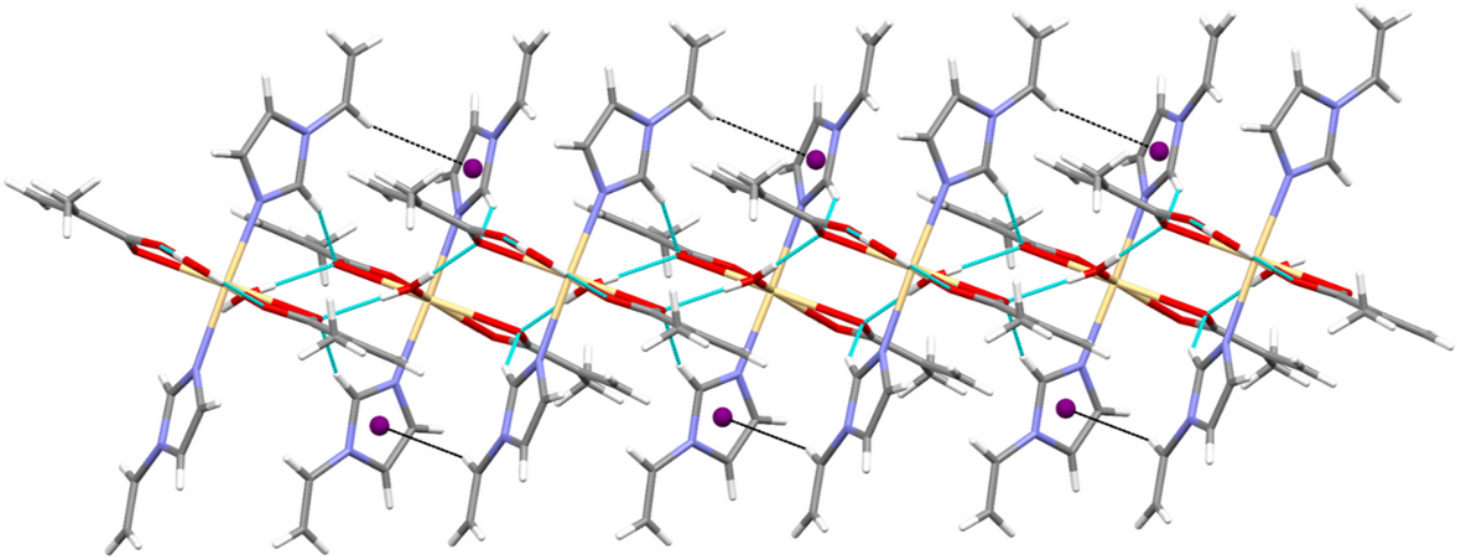

Figure 4

Inter-molecular C—H···π interactions of the complex

Figure 5

FT-IR spectrums of [Cd(maa)2(vim)2H2O]·H2O complex, maaH, and vim ligand

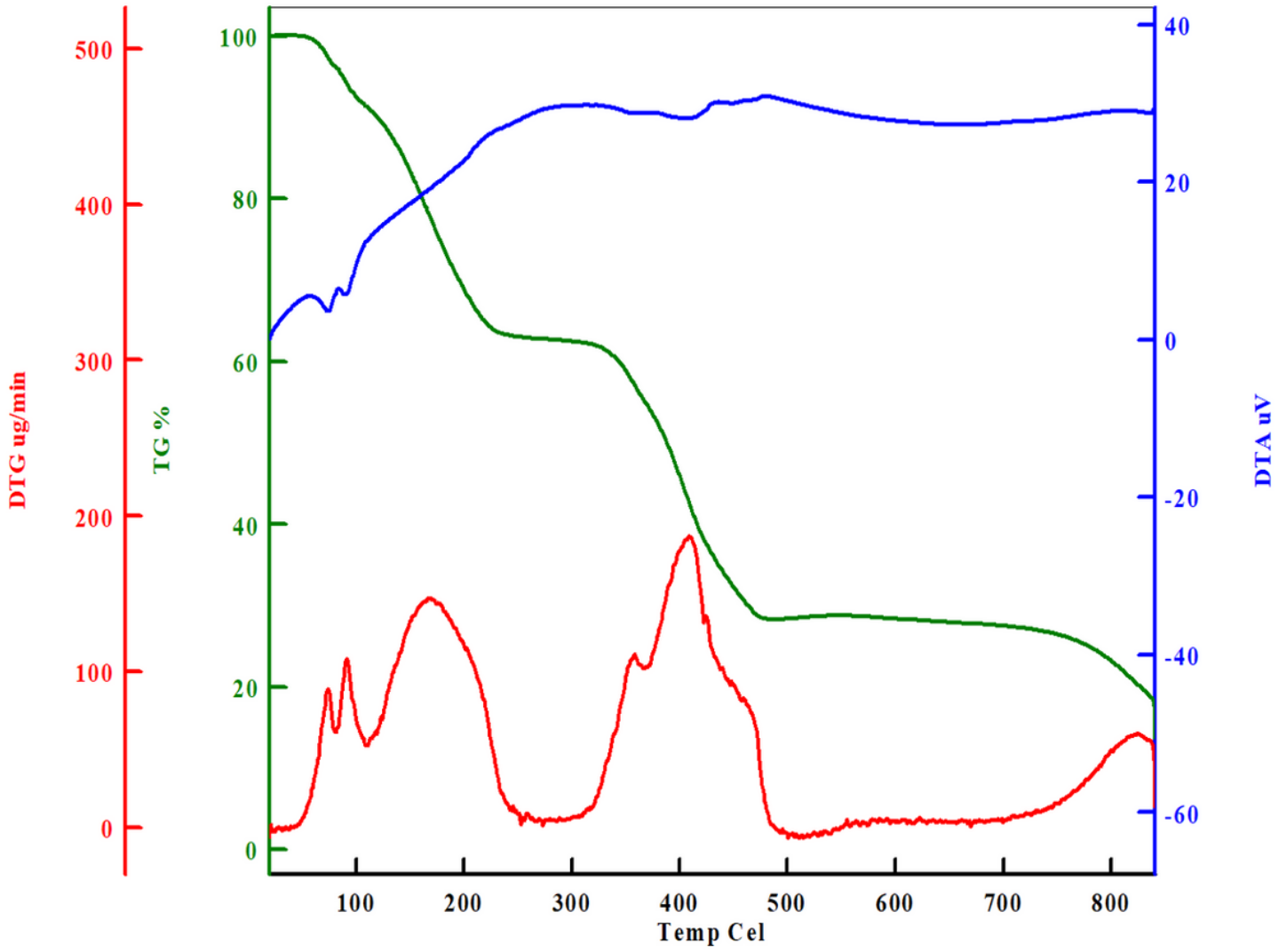

Figure 6

TGA curves of [Cd(maa)2(vim)2H2O]·H2O complex

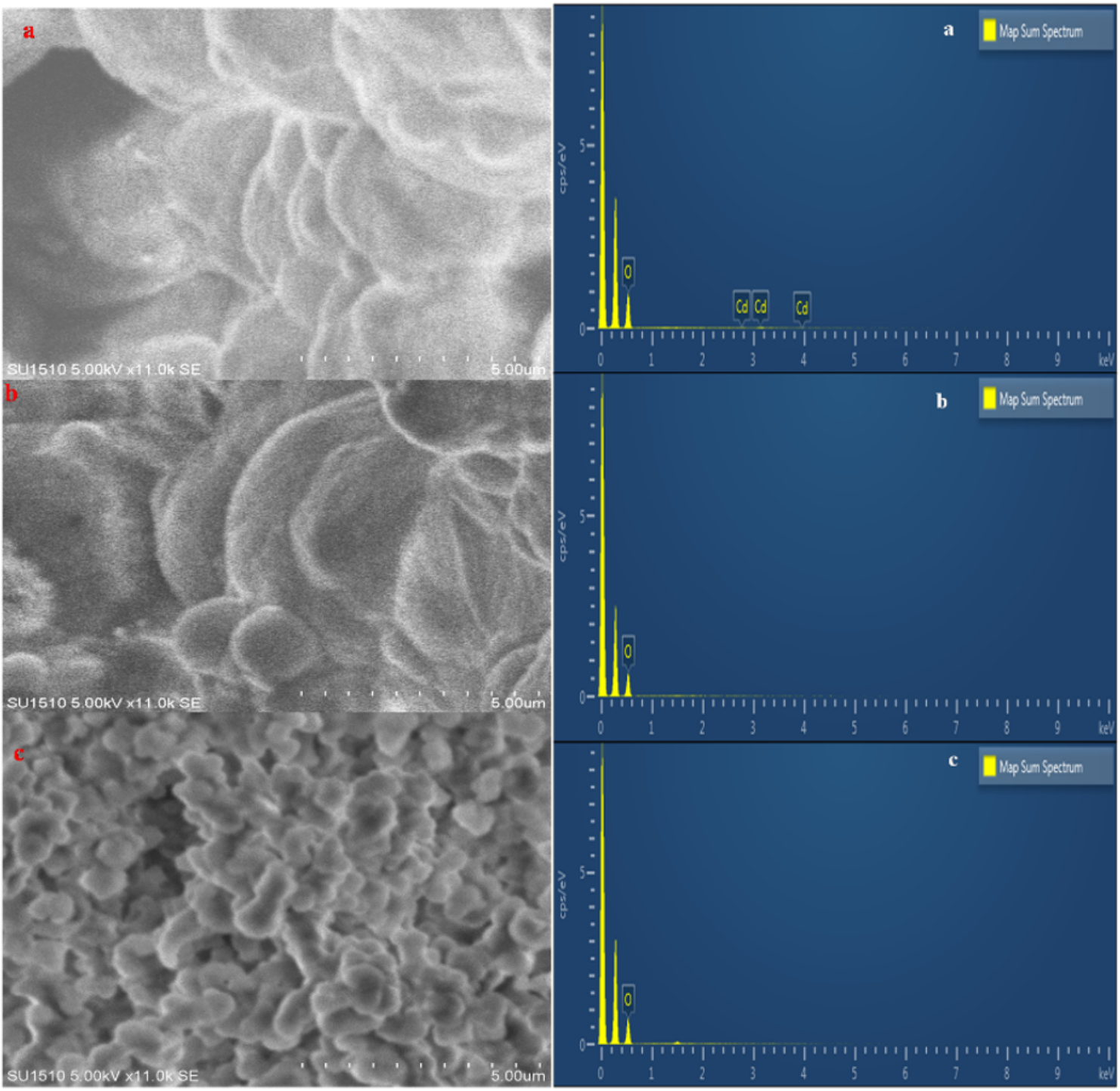

Figure 7

SEM-EDX spectrums of Cd(II)-IIP ((a) before elution (b) after elution) and NIP (c)

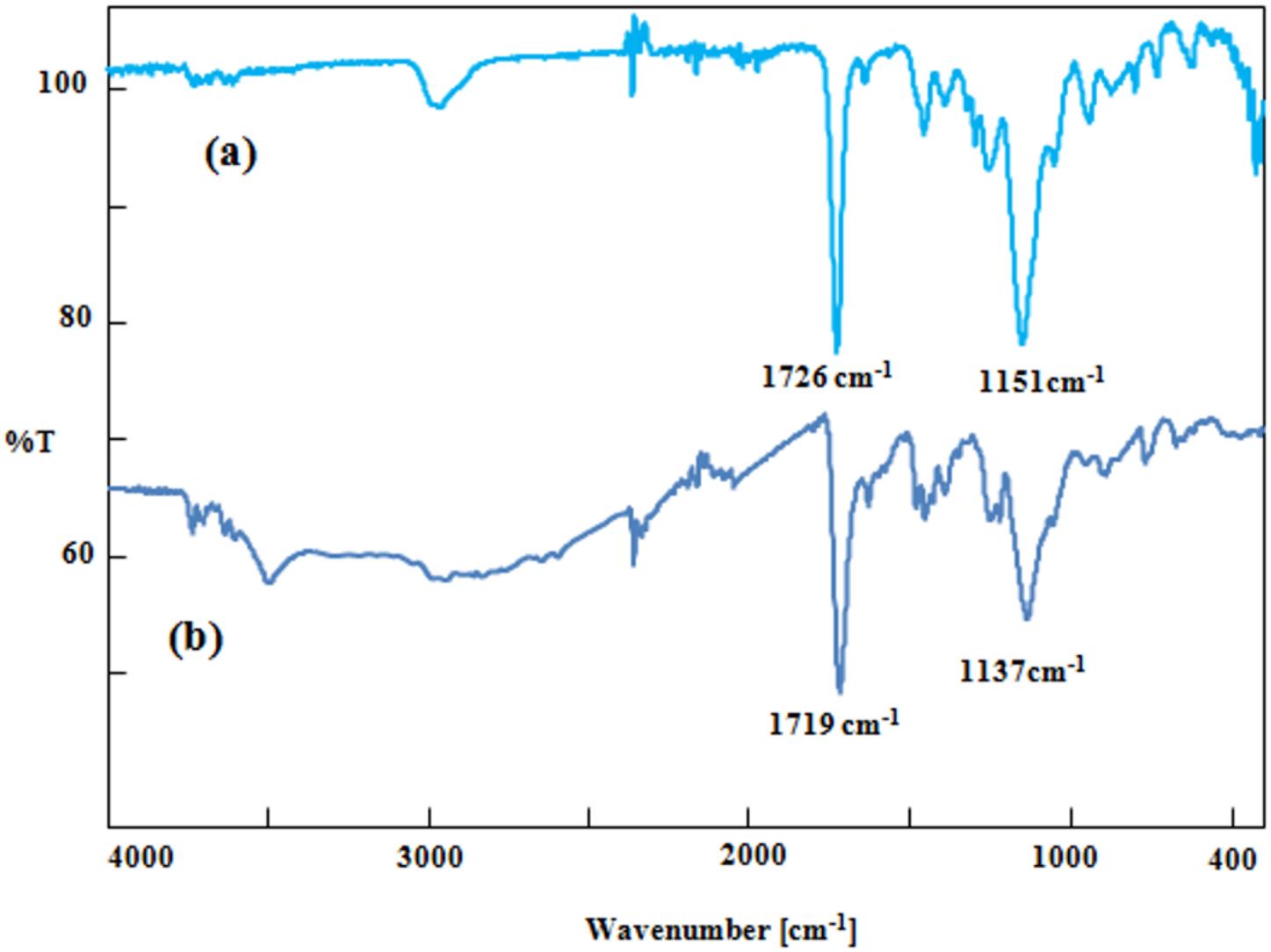

Figure 8

FT-IR spectrums of Cd(II)-IIP ((a) before elution, (b) after elution)

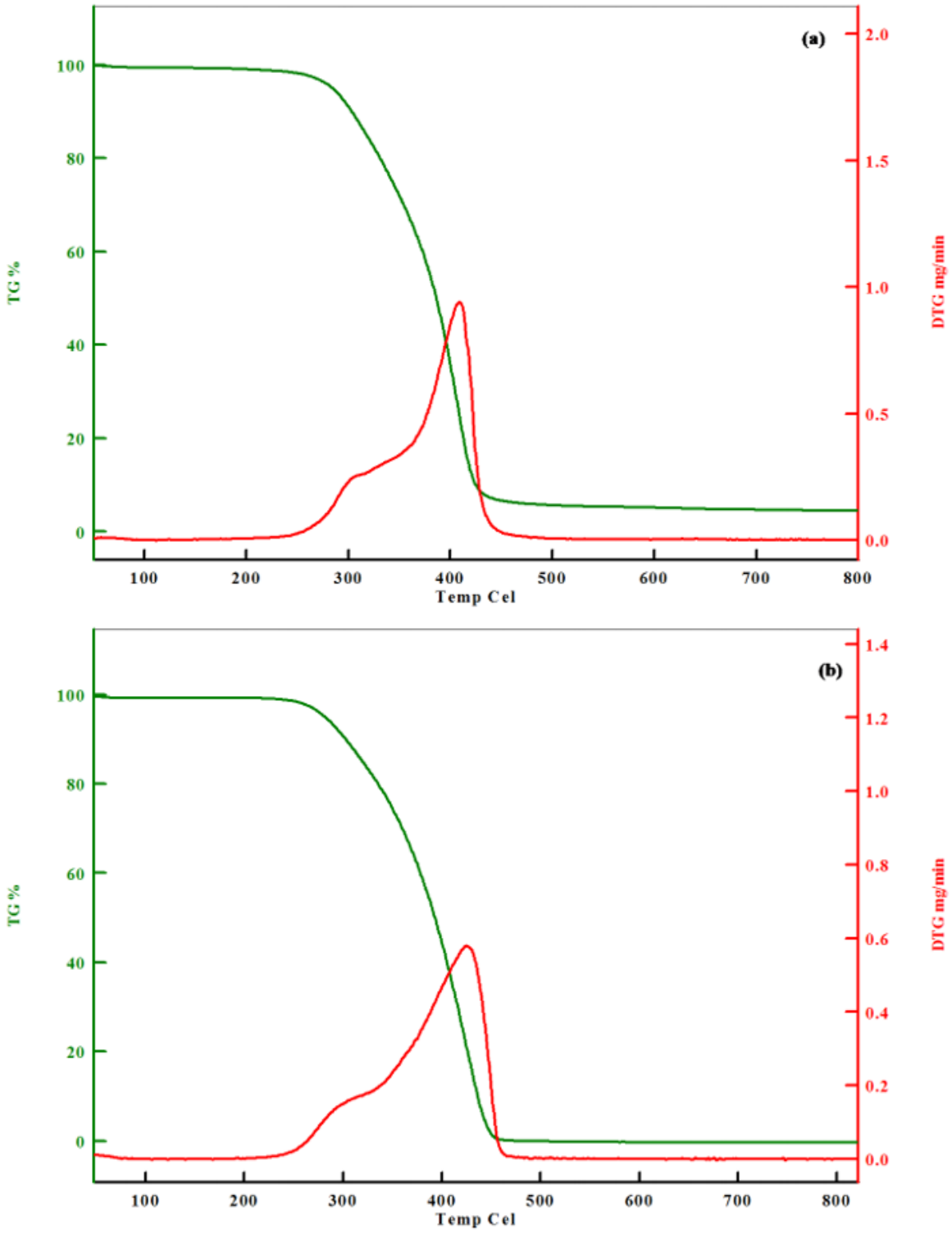

Figure 9

TGA curves of Cd(II)-IIP (a: before elution, b: after elution)

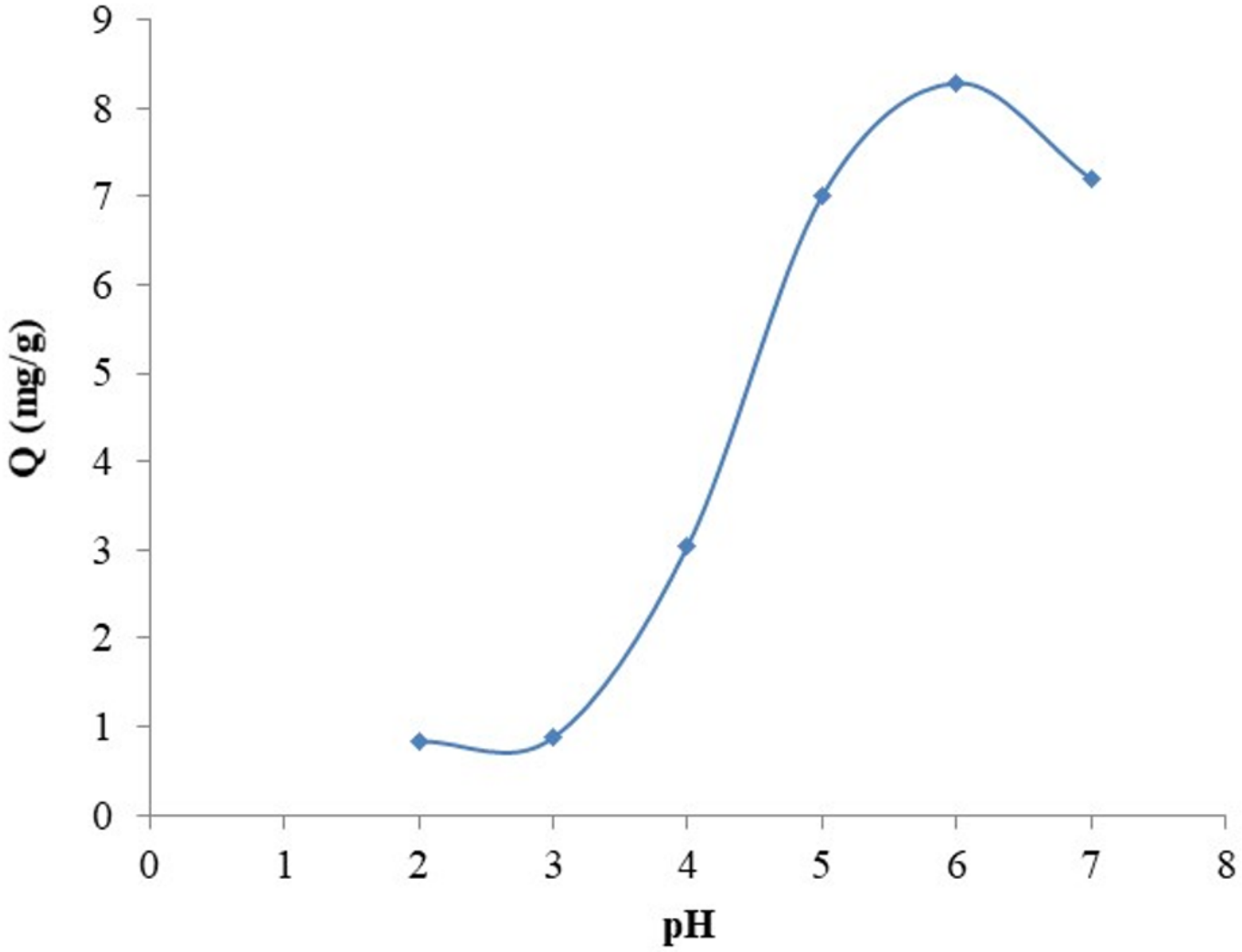

Figure 10

pH effect on adsorption capacity (50 ppm Cd(II), 50 mg Cd(II)-IIP, 24 h, 25 °C)

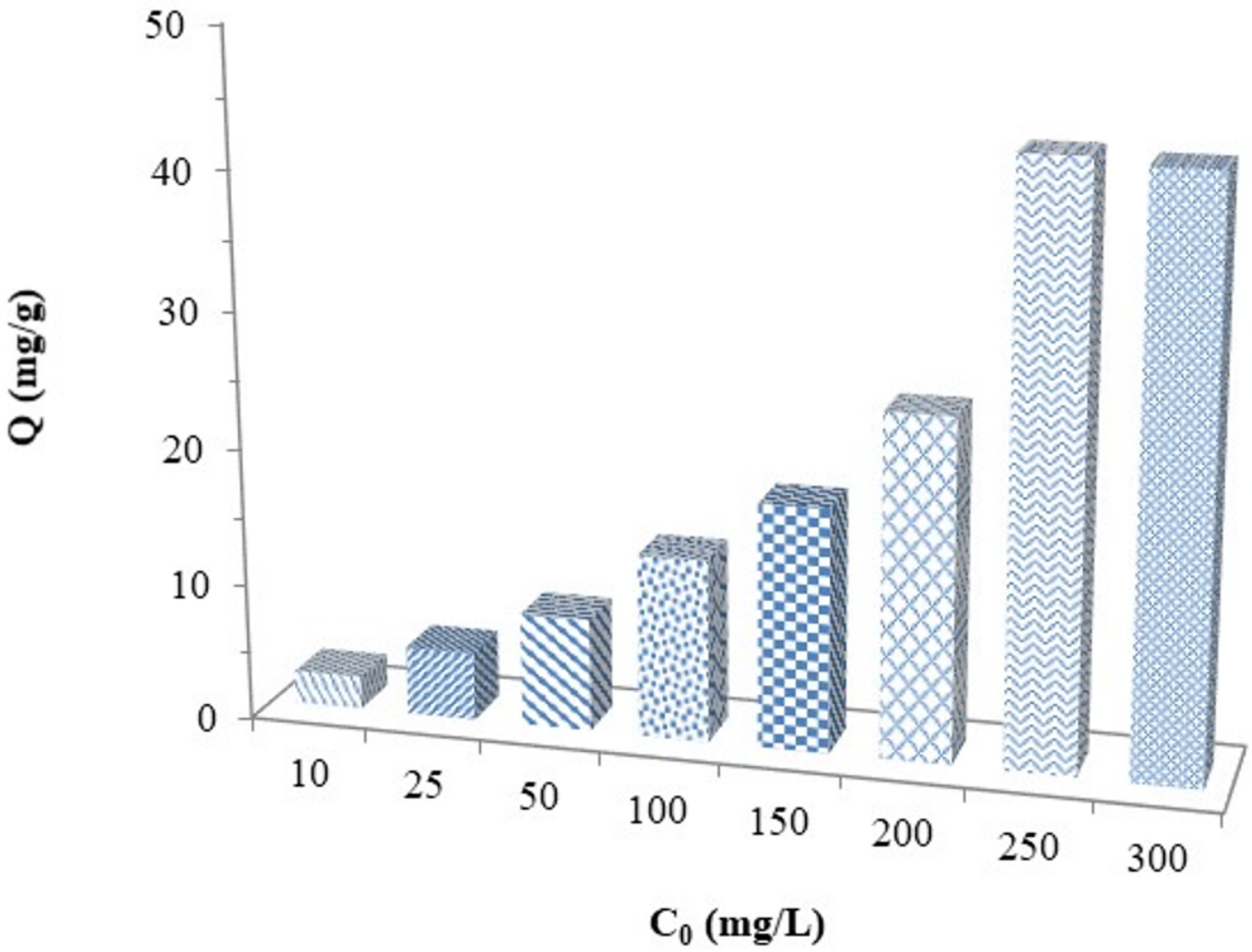

Figure 11

Effect of initial Cd(II) concentration (50 mg Cd-IIP, 24 h, 25 °C)

Supplementary Files

This is a list of supplementary files associated with this preprint. Click to download.

- Fig.S1.tif
- Fig.S2.tif
- SupplemantaryFile.docx